Neuropathological findings

Macroscopic findings

All three cases showed very similar macroscopic findings. The brain weights (840, 910 and 1010 g) were subnormal, and generalized cerebral gyral atrophy with frontal accentuation was observed. In coronal sections, the cerebral cortex was generally of normal color and thickness, whereas the cerebral white matter appeared grayish and was decreased in volume. The changes in the white matter were more prominent in the frontal and temporal lobes. The lateral ventricle was dilated bilaterally. The basal ganglia, especially the caudate nucleus, were reduced in size (Fig. 1), and the thalamus was atrophic in Cases 1 and 2 but unremarkable in Case 3. The cerebellum and brain stems were unremarkable.

Histological findings of the white matter

All three cases showed a very similar distribution of demyelination consistent with Nasu-Hakola disease. The cerebral white matter showed diffuse and symmetrical demyelination with scattered axonal spheroids, predominantly in the frontal and temporal lobes. Fibrillary gliosis was noted in the demyelinating lesions. The pyramidal tract of the pons and medulla oblongata was also involved.

Histological findings of the gray matter

Neuronal loss and gliosis

All three cases showed neuronal loss and gliosis in the thalamus, caudate nucleus, putamen and substantia nigra (Figs 2–6). The characteristics of the gray matter lesions were the same in each case and region: neuronal loss and reactive gliosis were prominent in the affected gray matter and the severity of gliosis correlated with the severity of neuronal loss. The distribution and severity of neuronal loss is shown in Table 2. Among these areas, the thalamus was most severely affected in all cases.

In the thalamus, the most severe neuronal loss and gliosis were found in the dorsomedial nucleus, followed by the anterior nucleus. Neuronal loss in the dorsomedial nucleus was severe in Case 1 (Fig. 2B,F) and Case 2 (Fig. 2C,G), and was moderate in Case 3 (Fig. 2D,H). Neuronal loss in the anterior nucleus was severe in Cases 1 and 2, but was not observed in Case 3. Neuronal loss in the ventrolateral nucleus was moderate in Cases 1 and 2, but was not observed in Case 3. The pulvinar nucleus showed moderate neuronal loss in Case 1, but could not be examined in Cases 2 and 3. Neuronal loss in the caudate nucleus was severe in Case 1 (Fig. 3B,F) and Case 2 (Fig. 3C,G), but mild in Case 3 (Fig. 3D,H). Neu-

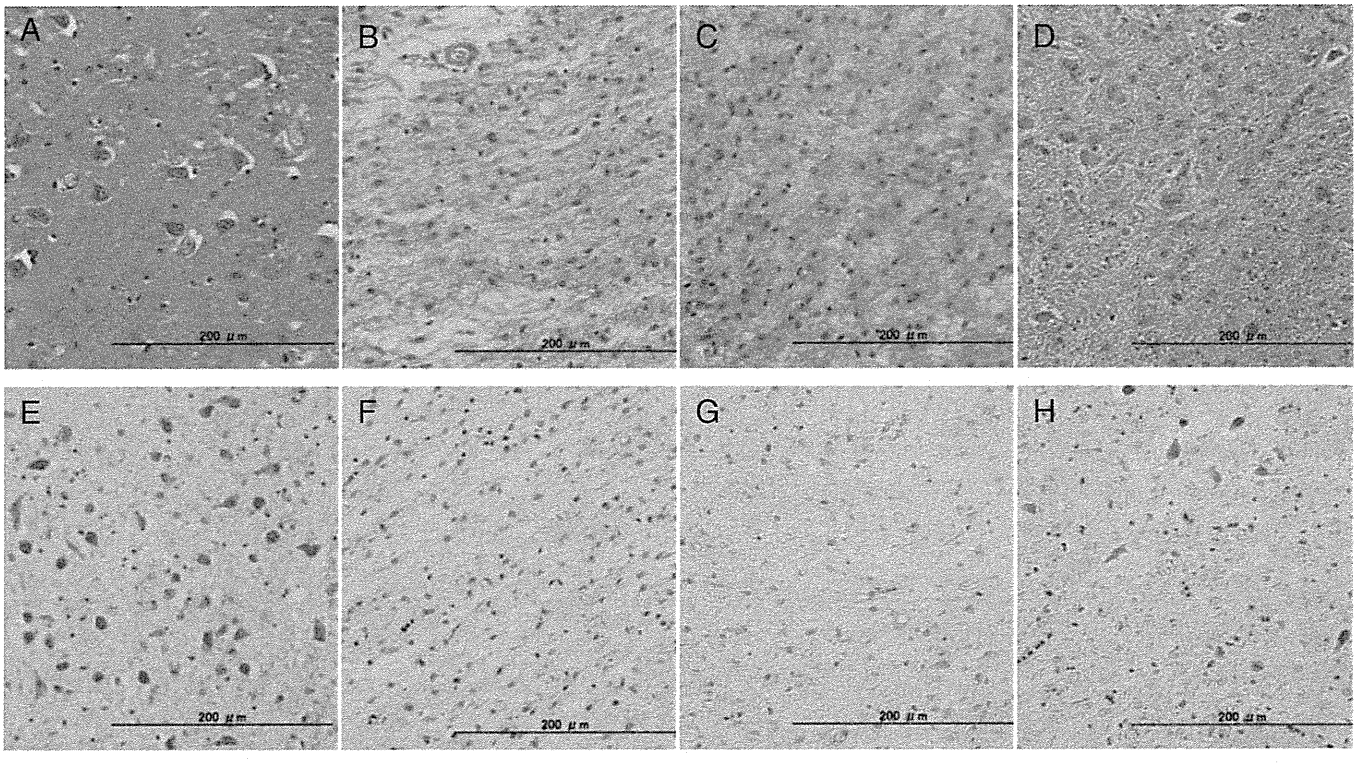

Fig. 2 Neuronal loss associated with glial proliferation in the thalamus (dorsomedial nucleus). Neither neuronal loss nor glial proliferation is noted in the normal control (A, E). Severe neuronal loss, remarkable glial proliferation, and tissue rarefaction are found in Case 1 (B, F) and Case 2 (C, G). Mild neuronal loss and glial proliferation are found, but no tissue rarefaction is seen in Case 3 (D, H). (A, D): HE stain; (E–H): KB stain. All scale bars = 200 μm.

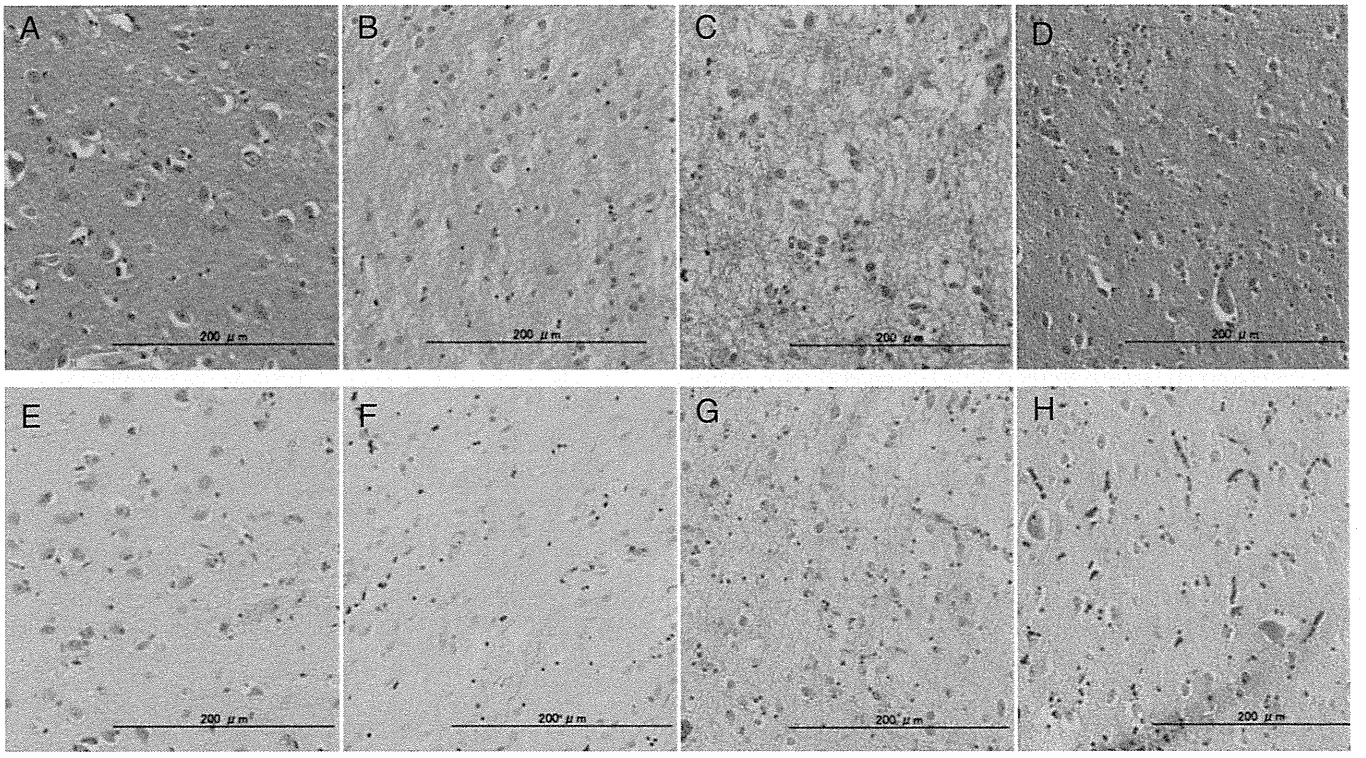

Fig. 3 Neuronal loss associated with glial proliferation in the caudate nucleus. Neither neuronal loss nor glial proliferation is noted in the normal control (A, E). Severe neuronal loss, remarkable glial proliferation, and tissue rarefaction are found in Case 1 (B, F) and Case 2 (C, G). Mild neuronal loss and glial proliferation are found, but no tissue rarefaction is seen in Case 3 (D, H). (A–D): HE stain; (E–H): KB stain. All scale bars = 200 μm.

ronal loss in the putamen was moderate in Case 1 (Fig. 4B,F) and Case 2 (Fig. 4C,G), but mild in Case 3 (Fig. 4D,H). Neuronal loss in the substantia nigra was moderate in Case 1 (Fig. 5B) and Case 2 (Fig. 5C), but mild in Case 3. The hippocampus showed severe neuronal loss in CA1, CA3 and the subiculum in Case 1, yet was preserved in Cases 2 and 3. The amygdaloid nucleus showed moderate neuronal loss in Case 1, with predominant involvement in the basolateral rather than the corticomedial area, but was preserved in Case 3 (Case 2 could not be examined). The cerebral cortex was relatively preserved in all cases. In the cerebellum, the cortex was almost normal, although a moderate loss of Purkinje cells was observed in Case 2.

Deposition of basophilic calcospherites

All three cases showed depositions of basophilic calcospherites, which were mainly found within the gray matter, such as the thalamus, caudate nucleus and putamen. While some calcospherites were located in perivascular sites as well as in blood vessel walls, most were not associated with blood vessels. Also, the calcospherites were not associated with gliosis or other pathological changes.

DISCUSSION

In the present study, we examined three cases of Nasu-Hakola disease in order to focus specifically on gray matter lesions. While genetic analysis was not performed, all the cases presented the typical pathology of the disease. Two types of neuropathology have been reported in Nasu-Hakola disease. One is characterized by marked demyelination, slight fibrillary gliosis and numerous sudanophilic deposits, a form of sudanophilic leukodystrophy. The other is characterized by marked fibrillary gliosis, slight demyelination, "dissociation glio-myelinique", and numerous spheroids in the cerebral white matter, a form of a sclerosing leukoencephalopathy.[10] The three cases addressed in this report belong to the latter type.

In addition to the characteristic degeneration of cerebral white matter, such as demyelination with conspicuous fibrillary gliosis and axonal changes, all three cases showed overt pathology in the gray matter. While the cerebral cortex was relatively preserved, neuronal loss and gliosis were observed in the thalamus (particularly in the dorsomedial nucleus and anterior nucleus), caudate nucleus, putamen and substantia nigra in all three cases. In addition, Case 1 showed neuronal loss and gliosis in the gray matter

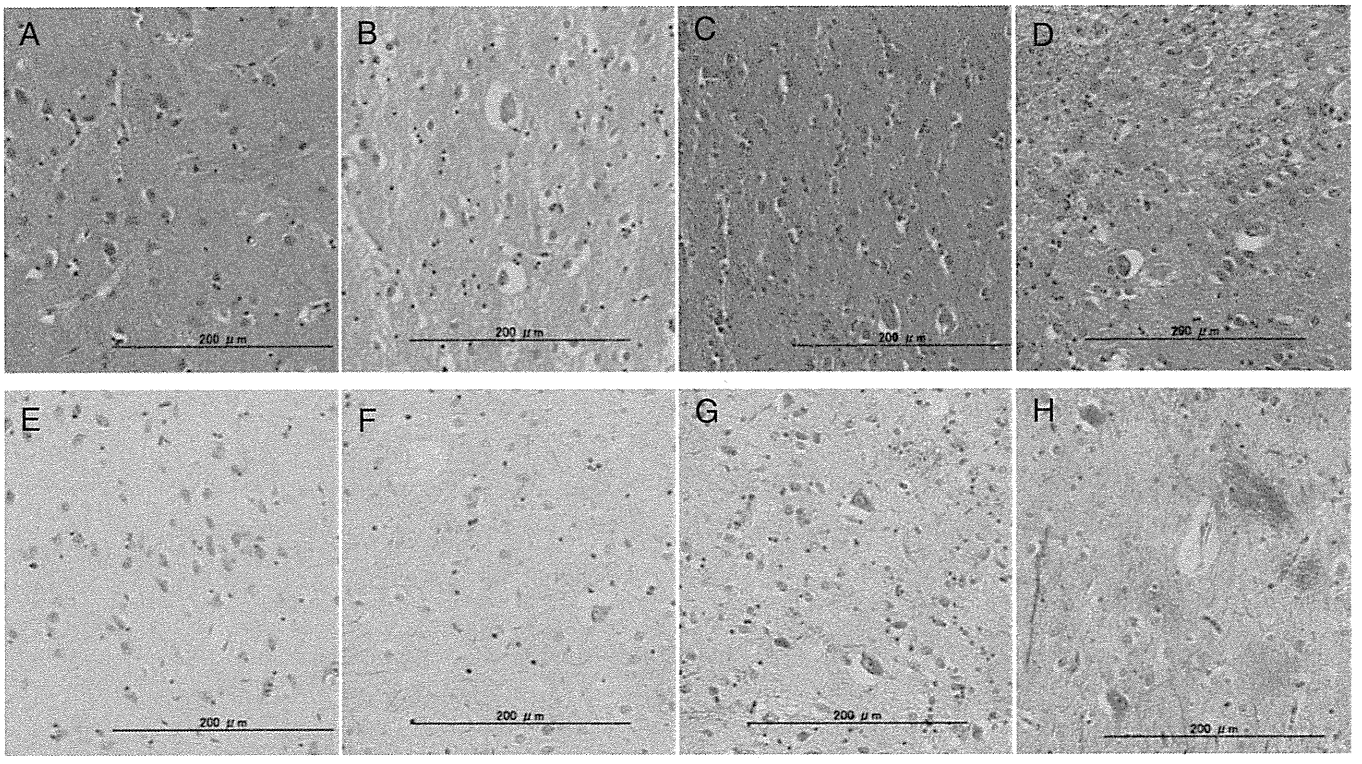

Fig. 4 Neuronal loss associated with glial proliferation in the putamen. Neither neuronal loss nor glial proliferation is noted in the normal control (A, E). Moderate neuronal loss and glial proliferation are found, but no tissue rarefaction is seen in Case 1 (B, F) and Case 2 (C, G). Mild neuronal loss and glial proliferation are found, but no tissue rarefaction is seen in Case 3 (D, H). (A–D): HE stain; (E–H): KB stain. All scale bars = 200 μm.

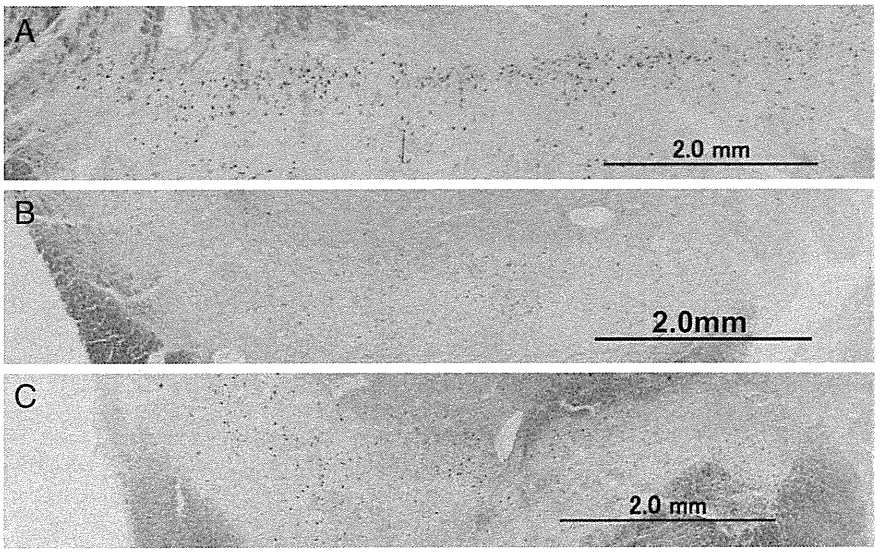

Fig. 5 The substantia nigra at low magnification. The number of neurons in Case 1 (B) and Case 2 (C) are moderately reduced, compared with the control (A). KB stain. All scale bars = 2.0 mm.

of the hippocampus and amygdala nucleus. Among the gray matter lesions, the thalamus was most severely affected. In Case 3, neuronal loss was generally mild, correlating with the shortest disease duration.

To date, gray matter lesions in Nasu-Hakola disease have been described in only a few reports.[11–14] Amano *et al.* reported a case showing neuronal loss in the thalamus (especially in the anterior and dorsomedial nucleus) and Purkinje cell layer, and astrocytosis in the putamen and globus pallidus. They reported that a long clinical course (33 years) and repeated episodes of convulsions might play a role in the lesions. Miyazu *et al.* also reported a case

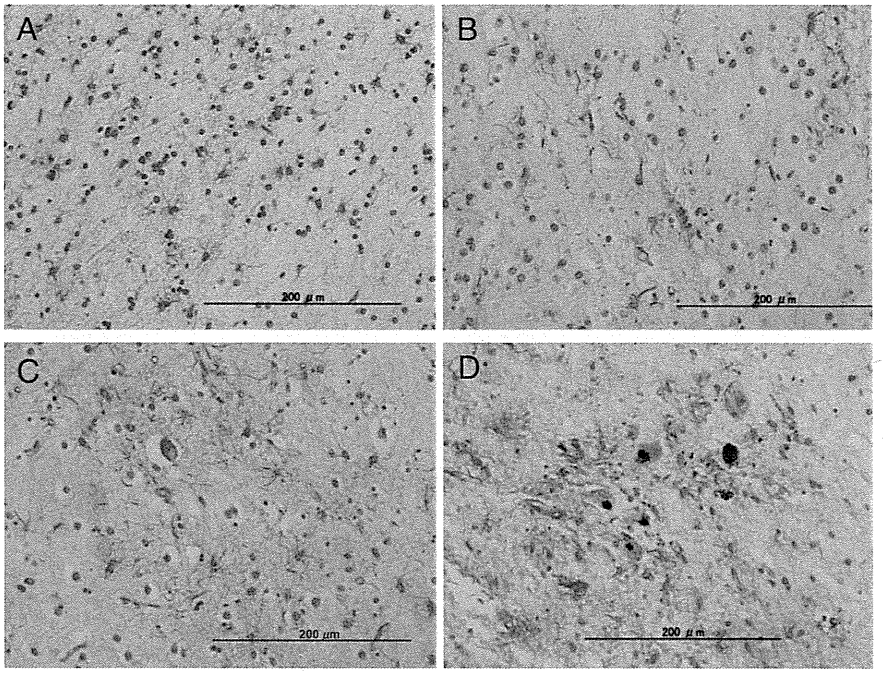

Fig. 6 Astrocytosis and gliosis in the thalamus (A), caudate nucleus (B), putamen (C) and substantia nigra (D). Holzer stain. All scale bars = 200 μm. (Case 1)

showing neuronal loss in the thalamus (particularly in the anterior, medial and pulvinar nucleus). Since this case experienced only a few episodes of convulsions and had a relatively short duration of disease, they considered the thalamic lesion to be a primary degeneration point. Paloneva *et al.* reported three cases showing neuronal loss in the thalamus, caudate nucleus and Purkinje cell layer, suggesting early basal ganglia involvement in this disease. The pathologies of the three cases described in this study corroborate the finding that neuronal loss is a constant feature of the thalamus and basal ganglia in Nasu-Hakola disease, while the neurons are relatively preserved in the cerebral cortex.

Although the precise pathomechanism underlying the gray matter lesions in Nasu-Hakola disease remains unknown, the following three factors are considered to be possible causes: dysfunction of the microglia, secondary changes due to axonal destruction, and convulsions. First, dysfunction of the microglia has been proposed to explain the CNS pathogenesis, since mutations in TREM2 and DAP12 have been identified as the primary causes of the disease.[5,6] Because microglia have the ability to phagocytose myelin,[15,16] the white matter may be severely damaged by abnormally activated microglia. Then the neuronal loss in the gray matter could be induced by defective functional activity in glial–neuronal interactions. Second, it is possible that the gray matter lesions are secondary changes due to axonal destruction in the white matter. In particular, the thalamus has many fiber connections with the frontal lobe through the white matter. While few reports focus on the gray matter lesions in other leukodystrophies, neuronal loss in the thalamus has frequently been reported.[17–19] For example, Tateishi *et al.* reported a case of adrenoleukodystrophy showing neuronal loss in the thalamus (particularly in the dorsomedial nucleus and anterior nucleus), the pontine nucleus, the inferior olivary nucleus and the cerebellar gray matter. Taken together with the distribution of white matter lesions, they concluded that the lesions were likely to be secondary changes in disruption of the thalamo-cortical, cerebro-ponto-cerebellar and olivocerebellar connections. Likewise, Schaumburg *et al.* reported that the dorsomedial nucleus and anterior nucleus of the thalamus were unremarkable in adrenoleukodystrophy cases lacking frontal lobe lesions.[20] Third, repeated episodes of epileptic convulsions may play a role in gray matter lesions, particularly in the hippocampus. The hippocampus is known to be vulnerable to epileptic convulsions, and hippocampal sclerosis is a characteristic neuropathological feature of epilepsy.[21] Among the cases presented here, the hippocampal gray matter lesions were most severe in Case 1, possibly corresponding to the history of more frequent convulsions than in the other two cases.

Among the remarkable clinical features seen in the present cases were the extrapyramidal symptoms in Case 1 (brachybasia and tremor) and Case 3 (brachybasia, rigidity and tremor), whereas a full neurological evaluation was not performed in Case 2 because of the multiple bone fractures. Although these symptoms can be considered to be a less prominent clinical manifestation than the other

symptoms, such as personality change, dementia and convulsions, only a few reports have described extrapyramidal symptoms in the clinical course of the disease.[3,22] Harada, for example, reported a case showing brachybasia, rigidity, masked face and tremor, and the case also exhibited atrophy in the basal ganglia. However, the origin of the symptoms of this disease remains unclear. In all the three cases presented here, neuronal loss was found in the basal ganglia as well as the substantia nigra, indicating that these may be responsible for the extrapyramidal symptoms. Nigro-striatal degeneration could be a constant pathological feature of Nasu-Hakola disease, at least in cases accompanied by extrapyramidal symptoms.

In conclusion, this study shows that the gray matter is commonly affected by neuronal loss and gliosis in Nasu-Hakola disease, with the exception of the cortical gray matter. These pathologies were prominent in the thalamus, caudate nucleus, putamen and substantia nigra, and the severity correlated with the disease duration in our series. These pathologies are considered to be responsible for some of the clinical manifestations of the disease, including the extrapyramidal symptoms.

ACKNOWLEDGMENTS

The authors thank Hiromi Kondo, Chie Haga and Yoko Shimomura for their expert technical support.

REFERENCES

1. Nasu T, Tsukahara Y, Terayama K, Mamiya N. An autopsy case of "membranous lipodystrophy" with myeloosteopathy of long bones and leucodystrophy of the brain. The 59th Tokyo Meeting of Pathology, Tokyo. *Tokyo Byori Shudankai Kiji* 1970; 10–13.
2. Hakola HPA, Järvi OH, Sourander P. Osteodysplasia polycystica hereditaria combined with sclerosing leucoencephalopathy, a new entity of the dementia praesenilis group. *Acta Neurol Scand Suppl* 1970; **43**: 78–79.
3. Hakola HPA. Neuropsychiatric and genetic aspects of a new hereditary disease characterized by progressive dementia and lipomembranous polycystic osteodysplasia. *Acta Psychiatr Scand Suppl* 1972; **232**: 1–173.
4. Pekkarinen P, Hovatta I, Hakola P *et al.* Assignment of the locus for PLO-SL, a frontal-lobe dementia with bone cysts, to 19q13. *Am J Hum Genet* 1998; **62**: 362–372.
5. Paloneva J, Kestilä M, Wu J *et al.* Loss-of-function mutations in TYROBP (DAP12) result in a presenile dementia with bone cysts. *Nat Genet* 2000; **25**: 357–361.
6. Paloneva J, Manninen T, Christman G *et al.* Mutations in two genes encoding different subunits of a receptor signaling complex result in an identical disease phenotype. *Am J Hum Genet* 2002; **71**: 656–662.
7. Bouchon A, Hernández-Munain C, Cella M, Colonna M. A DAP12-mediated pathway regulates expression of CC chemokine receptor 7 and maturation of human dendritic cells. *J Exp Med* 2001; **194**: 1111–1122.
8. Daws MR, Lanier LL, Seaman WE, Ryan JC. Cloning and characterization of a novel mouse myeloid DAP12-associated receptor family. *Eur J Immunol* 2001; **31**: 783–791.
9. Matsushita M, Oyanagi S, Hanawa S, Shiraki H, Kosaka K. Nasu-Hakola's disease (membranous lipodystrophy). A case report. *Acta Neuropathol* 1981; **54**: 89–93.
10. Sourander PA. New entity of phacomatosis:B.Brain lesions (Sclerosing leukoencephalopathy). *Acta Pathol Microbiol Scand Suppl* 1970; **215**: 44.
11. Amano N, Iwabuchi K, Sakai H *et al.* Nasu-Hakola's disease (membranous lipodystrophy). *Acta Neuropathol* 1987; **74**: 294–299.
12. Miyazu K, Kobayashi K, Fukutani Y *et al.* Membranous lipodystrophy (Nasu-Hakola disease) with thalamic degeneration: report of an autopsied case. *Acta Neuropathol* 1991; **82**: 414–419.
13. Kobayashi K, Kobayashi E, Miyazu K *et al.* Hypothalamic haemorrhage and thalamus degeneration in a case of Nasu-Hakola disease with hallucinatory symptoms and central hypothermia. *Neuropathol Appl Neurobiol* 2000; **26**: 98–101.
14. Paloneva J, Autti T, Raininko R *et al.* CNS manifestations of Nasu-Hakola disease: a frontal dementia with bone cysts. *Neurology* 2001; **56**: 1552–1558.
15. Mosley K, Cuzner ML. Receptor-mediated phagocytosis of myelin by macrophages and microglia: effect of opsonization and receptor blocking agents. *Neurochem Res* 1996; **21**: 481–487.
16. Smith ME. Phagocytosis of myelin by microglia in vitro. *J Neurosci Res* 1993; **35**: 480–487.
17. Tateishi J, Sato Y, Suetsugu M, Takashiba T. Adrenoleukodystrophy with olivopontocerebellar atrophy-like lesions. *Clin Neuropathol* 1986; **5**: 34–39.
18. Kakita A, Ishikawa A, Koike R, Tsuji S, Takahashi H. Adrenoleukodystrophy with involvement of the cerebral cortex. *Neuropathology* 1997; **17**: 106–111.
19. Sima AA, Pierson CR, Woltjer RL *et al.* Neuronal loss in Pelizaeus-Merzbacher disease differs in various mutations of the proteolipid protein 1. *Acta Neuropathol* 2009; **118**: 531–539.
20. Schaumburg HH, Powers JM, Raine CS, Suzuki K, Richardson EP Jr. Adrenoleukodystrophy. A clinical

and pathological study of 17 cases. *Arch Neurol* 1975; **32**: 577–591.
21. Fujikawa DG, Itabashi HH, Wu A, Shinmei SS. Status epilepticus-induced neuronal loss in humans without systemic complications or epilepsy. *Epilepsia* 2000; **41**: 981–991.
22. Harada K. A case of "membranous lipodystrophy (Nasu)" with emphasis on psychiatric and neuropathologic aspects (author's transl). *Folia Psychiatr Neurol Jpn* 1975; **29**: 169–177.

Communicative & Integrative Biology 4:4, 501-502; July/August 2011; ©2011 Landes Bioscience

In vitro recapitulation of aberrant protein inclusions in neurodegenerative diseases

New cellular models of neurodegenerative diseases

Takashi Nonaka* and Masato Hasegawa*

Laboratory of Neuropathology and Cell Biology; Tokyo Metropolitan Institute of Medical Science; Setagaya-ku, Tokyo Japan

Aberrant protein aggregates in affected brain cells of patients with neurodegenerative diseases are a well-known hallmark, but although the formation of these inclusions is an important pathogenic event, the mechanism involved remains unclear. We have recently established a simple method to introduce protein fibrils into cultured cells as seeds for protein aggregation, and we showed that intracellular soluble α-synuclein or tau can aggregate in cultured cells dependently upon seeds introduced in this way. Seeded aggregation of α-synuclein induced necrotic cell death, which was suppressed by the addition of various polyphenols. Our cellular models are expected to be valuable tools not only for elucidating the molecular mechanisms of onset of neurodegenerative diseases, but also for drug discovery.

Key words: alpha-synuclein, tau, intracellular aggregates formation, transduction of protein fibrils, cell death

Submitted: 04/06/11

Accepted: 04/07/11

DOI: 10.4161/cib.4.4.15779

*Correspondence to: Masato Hasegawa and Takashi Nonaka;
Email: hasegawa-ms@igakuken.or.jp and nonaka-tk@igakuken.or.jp

Addendum to: Nonaka T, Watanabe ST, Iwatsubo T, Hasegawa M. Seeded aggregation and toxicity of α-synuclein and tau: cellular models of neurodegenerative diseases. J Biol Chem 2010; 285:34885–98; PMID: 20805224; DOI: 10.1074/jbc.M110.148.

In patients with neurodegenerative disorders, intracellular aberrant protein inclusions are often found in the brain, including neurofibrillary tangles in Alzheimer's disease or Lewy bodies in Parkinson's disease and dementia with Lewy bodies. These aberrant protein aggregates are often observed in the most affected regions of diseased brains, suggesting they may cause neuronal cell death, leading to onset of these diseases. Tau and α-synuclein are well-known cytosolic proteins that are the main components of neurofibrillary tangles and Lewy bodies, respectively. They are soluble and natively unfolded proteins, and it remains unclear how they become aggregated in neuronal cells. Indeed, intracellular aggregate formation of these proteins does not occur when cultured cells are transfected with expression plasmids encoding these proteins. On the other hand, many in vitro studies using recombinant proteins, such as Abeta, tau, α-synuclein or poly glutamine-containing protein, have shown that these proteins are readily aggregated into fibrils in the presence of seeds for aggregation. These findings prompted us to examine whether seeds-dependent aggregation would occur in cultured cells. Thus, we aimed to introduce protein fibrils into cultured cells as seeds for aggregation.

Transfection of plasmid DNA into cultured cells is conducted routinely by the use of liposomes of polycationic and neutral lipids in water, based on the principle of cell fusion. Several commercially available reagents such as Lipofectoamine, Lipofectamine 2000 or FuGENE6 are available to efficiently transfect plasmid DNA into cultured cells. We tested whether these transfection reagents could transfect cultured SH-SY5Y cells not only with plasmid DNA, but also with protein fibrils. After much trial and error, we finally succeeded in transfecting α-synuclein fibrils into these cells using Lipofectamine reagent. We found that the introduced recombinant α-synuclein fibrils are phosphorylated at Ser129 in cultured cells, indicating that they had been introduced by Lipofectamine.[1] Interestingly, monomeric and oligomeric α-synuclein could not be introduced by the use of Lipofectamine. We applied for a patent covering the use of Lipofectamine for transduction of recombinant protein fibrils into cultured cells in 2005 (patents

pending in the United States: 12/086124, the European Union: 06834541.2 and Japan: 2007-549210). Recently, other groups have also reported introduction of fibrillar protein into cultured cells with or without specific reagents.[2-5]

Next, we examined whether intracellular α-synuclein can be aggregated dependently upon introduced seeds. When α-synuclein fibrils mixed with Lipofectamine were introduced into cells transiently expressing α-synuclein, phosphorylated and ubiquitinated α-synuclein inclusions (~10 μm in diameter) were observed by means of confocal laser microscopy, indicating that plasmid-derived soluble α-synuclein formed aggregates in the presence of exogenous α-synuclein fibrils in cells, and these inclusions resembled Lewy bodies in diseased brains. Others have also reported that α-synuclein fibrils seed the formation of Lewy body-like intracellular inclusions in cultured cells.[4] On the other hand, introduced tau fibrils were also shown to act as seeds for intracellular aggregation of plasmid-derived soluble tau protein. Interestingly, we found that fibrils composed of 3-repeat tau isoform serve as seeds for intracellular aggregation of soluble 3-repeat tau, but not soluble 4-repeat tau and fibrils of 4-repeat tau seed serve as seeds for aggregation of soluble 4-repeat tau, but not soluble 3-repeat tau. Likewise, introduction of α-synuclein fibrils did not elicit intracellular tau aggregation in cells and soluble α-synuclein did not form intracellular aggregates in the presence of any tau fibrils. These results clearly indicate that intracellular protein aggregation is highly dependent on the species of protein fibril seeds. Now, we are examining whether detergent-insoluble fractions prepared from several diseased brains can be introduced into cells by Lipofectamine and can serve as seeds for intracellular aggregate formation of soluble α-synuclein, tau or TDP-43.

Does the formation of these inclusions lead to cell death or toxicity? The answer is yes. We observed non-apoptotic cell death in cells harboring these inclusions. In these cells, proteasome activity was found to be significantly reduced. This suppression may be related to the cause of cell death. Furthermore, we showed that cell death in cells with α-synuclein inclusions is effectively suppressed by the addition of various small molecules to the culture medium; polyphenols such as exifone and gossypetin were the most effective, suggesting that these compounds may be possible new drugs for the treatment of neurodegenerative diseases.

Our study strongly supports a seed-dependent mechanism for the formation of the intracellular protein aggregates. Recently, the intercellular transfer of inclusions made of tau,[3,6] α-synuclein[2,7,8] and huntingtin[9] has been reported, suggesting the existence of mechanisms reminiscent of those by which prions spread through the nervous system. It remains to be clarified whether the incorporation of amyloid seeds into neurons or glial cells, as shown in our study, also occurs in vivo, but our results strongly suggest that extracellular aggregates may be taken up into neurons by endocytosis or under certain specific conditions. Therefore, it may be crucial to inhibit not only the production of intracellular amyloid seeds, but also their spread into extracellular space and their propagation. Vaccination against α-synuclein[10] or tau may be an effective treatment, together with the inhibition of intracellular aggregates formation with small-molecular compounds, for the therapy of neurodegenerative diseases.

References

1. Nonaka T, Watanabe ST, Iwatsubo T, Hasegawa M. Seeded aggregation and toxicity of α-synuclein and tau: cellular models of neurodegenerative diseases. J Biol Chem 2010; 285:34885-98.
2. Desplats P, Lee HJ, Bae EJ, Patrick C, Rockenstein E, Crews L, et al. Inclusion formation and neuronal cell death through neuron-to-neuron transmission of α-synuclein. Proc Natl Acad Sci USA 2009; 106:13010-5.
3. Frost B, Jacks RL, Diamond MI. Prion-like mechanisms in neurodegenerative diseases. J Biol Chem 2009; 284:12845-52.
4. Luk KC, Song C, O'Brien P, Stieber A, Branch JR, Brunden KR, et al. Exogenous α-synuclein fibrils seed the formation of Lewy body-like intracellular inclusions in cultured cells. Proc Natl Acad Sci USA 2009; 106:20051-6.
5. Waxman EA, Giasson BI. A novel, high-efficiency cellular model of fibrillar α-synuclein inclusions and the examination of mutations that inhibit amyloid formation. J Neurochem 2010; 113:374-88.
6. Clavaguera F, Bolmont T, Crowther RA, Abramowski D, Frank S, Probst A, et al. Transmission and spreading of tauopathy in transgenic mouse brain. Nat Cell Biol 2009; 11:909-13.
7. Li JY, Englund E, Holton JL, Soulet D, Hagell P, Lees AJ, et al. Lewy bodies in grafted neurons in subjects with Parkinson's disease suggest host-to-graft disease propagation. Nat Med 2008; 14:501-3.
8. Kordower JH, Chu Y, Hauser RA, Freeman TB, Olanow CW. Lewy body-like pathology in long-term embryonic nigral transplants in Parkinson's disease. Nat Med 2008; 14:504-6.
9. Ren PH, Lauckner JE, Kachirskaia I, Heuser JE, Melki R, Kopito RR. Cytoplasmic penetration and persistent infection of mammalian cells by polyglutamine aggregates. Nat Cell Biol 2009; 11:219-25.
10. Masliah E, Rockenstein E, Adame A, Alford M, Crews L, Hashimoto M, et al. Effects of alpha-synuclein immunization in a mouse model of Parkinson's disease. Neuron 2005; 46:857-68.

Meyerowitz et al. Molecular Neurodegeneration 2011, 6:57
http://www.molecularneurodegeneration.com/content/6/1/57

MOLECULAR NEURODEGENERATION

RESEARCH ARTICLE Open Access

C-Jun N-terminal kinase controls TDP-43 accumulation in stress granules induced by oxidative stress

Jodi Meyerowitz[1†], Sarah J Parker[1†], Laura J Vella[2], Dominic CH Ng[3,4], Katherine A Price[1], Jeffrey R Liddell[1], Aphrodite Caragounis[1], Qiao-Xin Li[1,5], Colin L Masters[5], Takashi Nonaka[6], Masato Hasegawa[6], Marie A Bogoyevitch[3,4], Katja M Kanninen[1], Peter J Crouch[1] and Anthony R White[1*]

Abstract

Background: TDP-43 proteinopathies are characterized by loss of nuclear TDP-43 expression and formation of C-terminal TDP-43 fragmentation and accumulation in the cytoplasm. Recent studies have shown that TDP-43 can accumulate in RNA stress granules (SGs) in response to cell stresses and this could be associated with subsequent formation of TDP-43 ubiquinated protein aggregates. However, the initial mechanisms controlling endogenous TDP-43 accumulation in SGs during chronic disease are not understood. In this study we investigated the mechanism of TDP-43 processing and accumulation in SGs in SH-SY5Y neuronal-like cells exposed to chronic oxidative stress. Cell cultures were treated overnight with the mitochondrial inhibitor paraquat and examined for TDP-43 and SG processing.

Results: We found that mild stress induced by paraquat led to formation of TDP-43 and HuR-positive SGs, a proportion of which were ubiquitinated. The co-localization of TDP-43 with SGs could be fully prevented by inhibition of c-Jun N-terminal kinase (JNK). JNK inhibition did not prevent formation of HuR-positive SGs and did not prevent diffuse TDP-43 accumulation in the cytosol. In contrast, ERK or p38 inhibition prevented formation of both TDP-43 and HuR-positive SGs. JNK inhibition also inhibited TDP-43 SG localization in cells acutely treated with sodium arsenite and reduced the number of aggregates per cell in cultures transfected with C-terminal TDP-43 162-414 and 219-414 constructs.

Conclusions: Our studies are the first to demonstrate a critical role for kinase control of TDP-43 accumulation in SGs and may have important implications for development of treatments for FTD and ALS, targeting cell signal pathway control of TDP-43 aggregation.

Keywords: TDP-43, stress granules, JNK, kinases, oxidative stress, paraquat, hnRNP

Background

Amyotrophic lateral sclerosis (ALS) is a fatal adult-onset neurodegenerative disease in which the function of motor neurons in the spinal cord and brain progressively deteriorates. ALS is by far the most prevalent form of motor neuron disease. Patients with ALS rarely survive more than 3-5 years after diagnosis with respiratory failure the most common cause of death [1]. Approximately 5% of patients with ALS have a positive family history of the disorder. The first pathological mutations identified in ALS were in superoxide dismutase 1 (SOD1) and account for around 20% of familial ALS cases [2]. That discovery has been the basis for most ALS research in the past decade, and animal models containing SOD1 mutant transgenes have provided important insights into SOD1-mediated neurotoxic effects. However, SOD1 mutations only account for 1-2% of all ALS cases [3].

* Correspondence: arwhite@unimelb.edu.au
† Contributed equally
[1]Department of Pathology, The University of Melbourne, Victoria, 3010, Australia
Full list of author information is available at the end of the article

Frontotemporal dementia (FTD) is the second most common cause of presenile dementia, affecting people in their 50s and 60s [4,5]. There are several clinical phenotypes and the historical neuropathological classification included either frontotemporal lobar degeneration with tau positive (FTLD-tau) or ubiquitin-positive (FTLD-U) inclusions [4,5]. The observation that some ALS patients developed cognitive deficits with frontal lobe degeneration resembling FTLD-U has led to the belief that ALS and FTD with FTLD-U might involve a clinical spectrum of neurodegenerative illnesses [5].

In 2006, TAR DNA binding protein 43 (TDP-43) was identified as the major protein constituent of ubiquitinated neuronal inclusions in FTLD-U and in non-SOD1 ALS cases [6,7]. This led to the re-classification of FTLD-U to FTLD-TDP-43, and TDP-43-positive ALS and FTLD-TDP-43 cases are now referred to collectively as primary TDP-43 proteinopathies [8]. These findings also provided further support for the concept of FTD and ALS as diseases within the same broad clinical spectrum. Subsequently, TDP-43-positive inclusions have been identified in a number of neurodegenerative diseases. In these cases, the TDP-43 identification is referred to as a secondary TDP-43 proteinopathy [8]. While the role of abnormal TDP-43 accumulation in both primary and secondary TDP-43 proteinopathies is not yet fully understood, the identification of TDP-43 mutations associated with ALS and FTD (~40 at present) has provided clear evidence that altered TDP-43 processing can be a primary cause of neurodegeneration and is not just a secondary phenomenon [9,10].

TDP-43 is a 414 amino acid protein of the heterogeneous nuclear ribonucleoprotein (hnRNP) family and consists of two RNA recognition motifs and a C-terminal glycine rich region [8,11]. It has a number of reported roles including transcription, pre-mRNA splicing, and transport and stabilization of mRNA [8]. The protein is normally localized to the nucleus and has a classical bipartite nuclear localization sequence [12]. TDP-43 contains two caspase 3 consensus cleavage sites leading to formation of C-terminal fragments (CTFs) of 35 kDa and 25 kDa that are excluded from the nucleus [8]. The majority of TDP-43 mutations occur in the C-terminal region and CTFs are commonly identified in ALS and FTD inclusions.

In post-mortem tissue from ALS and FTD, the hallmark neuropathological features include loss of TDP-43 expression in the nucleus together with accumulation of TDP-43 in cytoplasmic inclusions. These inclusions are enriched in ubiquitinated and hyperphosphorylated (phospho-Ser409/410) TDP-43 and there can be substantial enrichment of CTF-TDP-43 [8,11]. Recent cell studies have shown that transfection with CTF-TDP-43 can accurately re-capitulate the histopathological findings of ALS and FTD with accumulation of cytosolic ubiquitinated and phosphorylated CTF-TDP-43 aggregates [13-15]. In addition, transfection with these constructs can result in neurotoxicity and cell death although the pathways involved are not known [14].

However, while these studies have recapitulated findings of post-mortem disease tissue, they have told us little of the early disease processes associated with abnormal TDP-43 metabolism, particularly in sporadic TDP-43 proteinopathies which account for > 90% of ALS (and FTD) cases. A new insight into TDP-43 accumulation is developing through studies identifying TDP-43 association with RNA stress granule proteins [16,17]. Stress granules (SGs) are cytoplasmic sites of stalled mRNA pre-initiation complexes induced by oxidative changes, heat shock or osmotic stress where the cell stalls mRNA translation of non-critical proteins to shift energy expenditure to key repair and survival proteins [18]. Recent studies have shown that under stress, TDP-43 is recruited to SGs in a variety of cells [16,17,19,20]. Initially Moisse et. al. [21] reported that TDP-43 localized to SGs after axotomy in mice. Subsequently, studies in cells revealed that acute cell stress induced TDP-43 SG association and this was dependent on residues 216-315 and the first RNA recognition motif [19]. While the same group reported a lack of TDP-43 association with SG markers in ALS tissues, subsequent work by Volkening et al. [22] reported an association between TDP-43 and staufen in ALS spinal cord tissue. TDP-43 SG co-localization in ALS and FTLD-U has since been reported by Liu-Yesucevitz et al., [17] and FUS, another hnRNP protein associated with ALS, has also been identified in ALS SGs [23,24]. Liu-Yesucevitz et al. [17] also reported that TDP-43 may associate with SGs through interaction with SG proteins such as TIA-1 and this has been supported by studies on TDP-43 association with a number of SG proteins [20,25]

However, while these studies have advanced our understanding of the early stages of TDP-43 aggregation, the majority of this research has been performed in cells exposed to acute and highly toxic treatment with sodium arsenite, the standard means of inducing SGs [17,19,20]. In addition, much of our knowledge has been gained through generation of CTF-TDP-43 over-expression in transfected cells. There is a lack of understanding about the processes involved in endogenous TDP-43 aggregation during chronic oxidative stress. As the majority of ALS and FTD cases involve no known mutation in TDP-43 and the slow disease process characteristic of neurodegeneration involves chronic oxidative and nitrosative stresses [2,26], it is critical to determine how these factors affect TDP-43 SG cytosolic accumulation. Moreover, SG proteins have a high propensity to aggregate and over-expression of highly aggregating CTF

fragments may not accurately re-capitulate the underlying mechanistic processes involved in endogenous TDP-43 aggregation and association with SGs during chronic stress. Therefore, we investigated the effects of mild, chronic oxidative and nitrosative stress on endogenous TDP-43 in neuronal-like cell cultures. Our findings revealed that in contrast to acute stress, chronic oxidative stress induced several features consistent with TDP-43 proteinopathies including loss of nuclear TDP-43, accumulation of diffuse TDP-43 in the cytosol, formation of a 35 kDa C-terminal fragment and accumulation of TDP-43 in SGs, some of which revealed ubiquitination. Importantly, our findings revealed that TDP-43 localization to SGs was controlled by c-Jun N-terminal kinase (JNK). Inhibition of JNK also modulated TDP-43 accumulation in SGs induced by sodium arsenite and in cells transfected with CTF-TDP-43 constructs. Our data also indicated that the aggregation of TDP-43 may be associated with JNK modulation of hnRNP-TDP-43 interactions and SG localization.

Results

To investigate the effects of chronic stress on TDP-43 metabolism, we first determined optimal concentrations of oxidative and nitrosative stress inducers in SH-SY5Y neuronal-like cultures. Cells were treated overnight with each compound at a range of concentrations and the cell viability was determined by MTT assay and cell death was measured using an LDH assay (not shown). Additional File 1 shows the selected concentrations used for further investigation. The concentrations shown in Additional File 1 induced mild but significant reductions in cell viability overnight. However, except for 2 mM paraquat (24 ± 3.2% cell death) and 75 μM rotenone (32 ± 4.6% cell death), no change to LDH release was observed compared to untreated controls. These doses were used to mimic sub-lethal chronic stress conditions relevant to brain or spinal cord neurons during disease *in vivo*.

Nitrosative stress inducers mediate altered TDP-43 processing

Treatment of SH-SY5Y cells with inducers of nitrosative stress resulted in changes to sub-cellular distribution of TDP-43. Compared to untreated controls (Figure 1A-C), SIN-1, a peroxynitrite donor caused a frequent, evenly distributed, diffuse accumulation of TDP-43 in the cytosol of treated cells (Figure 1D-F). In contrast, paraquat, an inhibitor of the mitochondrial electron transport chain and inducer of superoxide/peroxynitrite stress (a common feature in neurodegeneration), induced substantial and varied cytoplasmic accumulation of TDP-43 including aggregates of TDP-43 resembling RNA SGs (Figure 1G-I). Arginine (nitric oxide precursor) had no consistent effect (Figure 1J-L).

Paraquat induces a robust cell model of TDP-43 proteinopathy

Further examination of TDP-43 in paraquat-treated cells revealed multiple features reported for human TDP-43 proteinopathies. Paraquat-treated cells frequently showed clear loss of nuclear TDP-43 (Figure 2D-F), accumulation of diffuse TDP-43 in the cytosol (Figure 2G-I) and formation of cytoplasmic aggregates. Interestingly, these changes were not always observed in the same cells suggesting that loss of nuclear TDP-43 expression and accumulation in the cytosol may been caused by different stress-mediated processes. To determine if the cytosolic aggregates of TDP-43 induced by paraquat were SGs, cells were co-stained for the SG marker, HuR. The majority of TDP-43 aggregates co-localized with HuR although there were also additional HuR-positive SGs that lacked TDP-43 (Figure 2N-Q). Quantitative analysis revealed that 66 ± 8% of paraquat-induced SGs that were positive for HuR were also positive for TDP-43 and that SG formation correlated to increasing toxicity of paraquat (Additional File 2). TDP-43 also frequently co-localized with the SG marker, TIA-1 (data not shown). We examined the time course of TDP-43 SG formation and found that TDP-43 only accumulated into SGs between 8 and 20 hr after exposure to paraquat. This is in contrast to the rapid accumulation of TDP-43 into SGs reported for arsenite or osmotic stress [19,20]. Our findings were also observed in retinoic-acid differentiated SY5Y neuronal-like cells, confirming that these changes can occur in non-dividing SY5Y cells (Additional File 2H-K).

We extended the investigation of this model further by examining if TDP-43-positive SGs revealed presence of the protein aggregate marker ubiquitin, also a hallmark feature of the ubiquitinated inclusions in ALS and FTLD-U in FTD. Interestingly, our study revealed that a number of the TDP-43-positive SGs co-localized with ubiquitin (Figure 3F and 3J). 24 ± 6% of TDP-43-positive SGs were also positive for ubiquitin indicating that only a portion of the SGs may progress to ubiquitinated protein aggregates (Figure 3). Diffuse TDP-43 did not consistently co-localize with ubiquitin (Figure 3J). Whether the ubiquitination of the SGs was associated directly with the TDP-43 or ubiquitination of alternative SG proteins is uncertain. Due to the relatively low numbers of cells containing ubiquitinated SGs and lack of a method for purifying SGs, it was not possible to determine if the ubiquitinated protein in the SGs was specifically TDP-43.

Interestingly, we did not observe phosphorylated TDP-43 associated with the SGs (Additional File 3A-F). This was confirmed by Western blot analysis that detected no increase in phosphorylated TDP-43 or phosphorylated CTF-TDP-43 post-exposure to paraquat

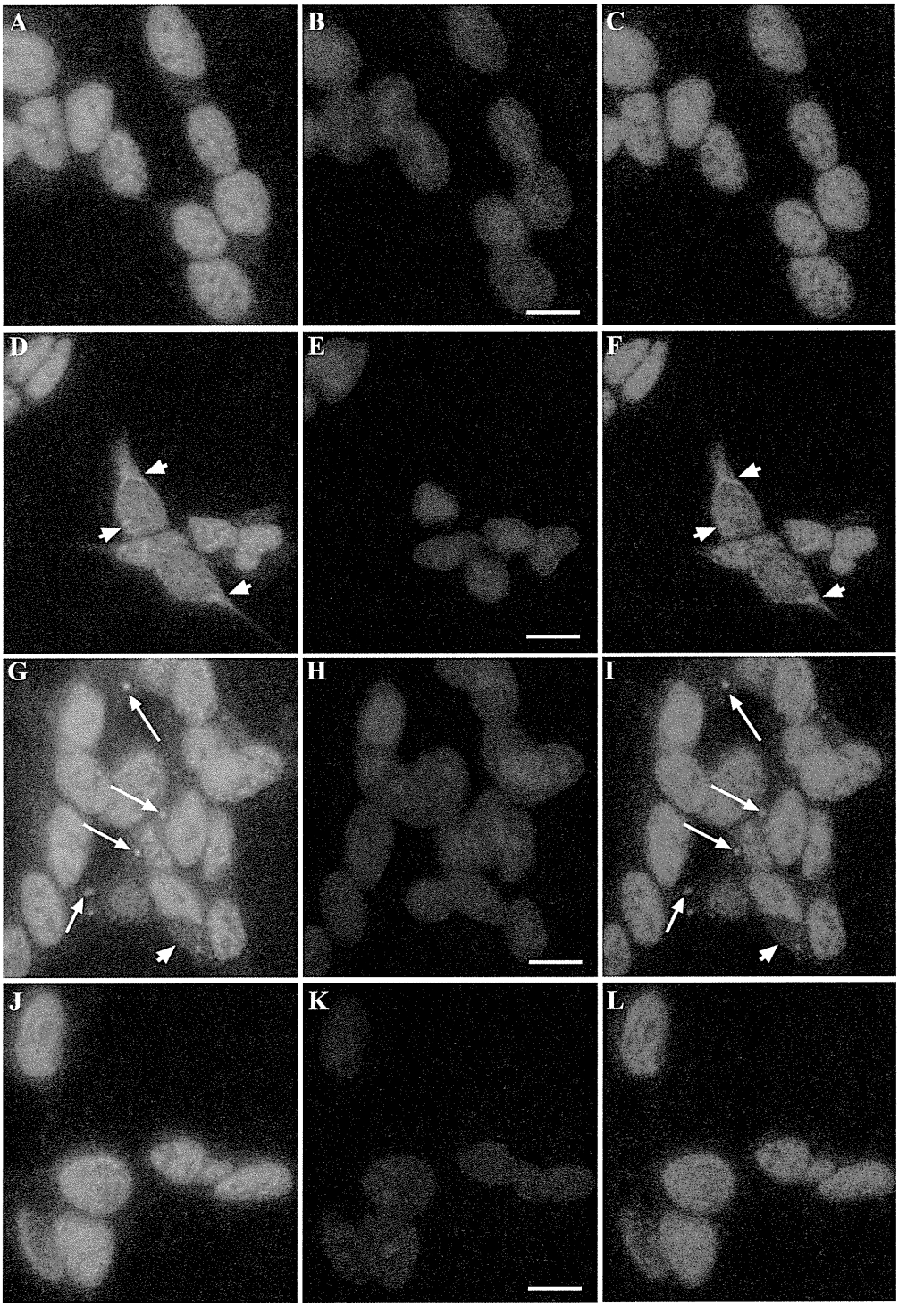

Figure 1 Effect of SIN-1, paraquat and arginine on TDP-43 localization in SH-SY5Y cells. Cells were exposed overnight with 0.1 mM SIN-1, 1 mM paraquat or 1 mM arginine and TDP-43 localization was examined by immunofluorescence. **A-C**: untreated, **D-F**: SIN-1, **G-I**: paraquat, **J-L**: arginine. Green = TDP-43, blue = DAPI. Right-hand panel = merged images of TDP-43 and DAPI. Arrowheads show diffuse cytosolic TDP-43. Arrows show aggregated cytosolic TDP-43. Bar = 10 μm. Representative images from three separate experiments performed in duplicate or triplicate.

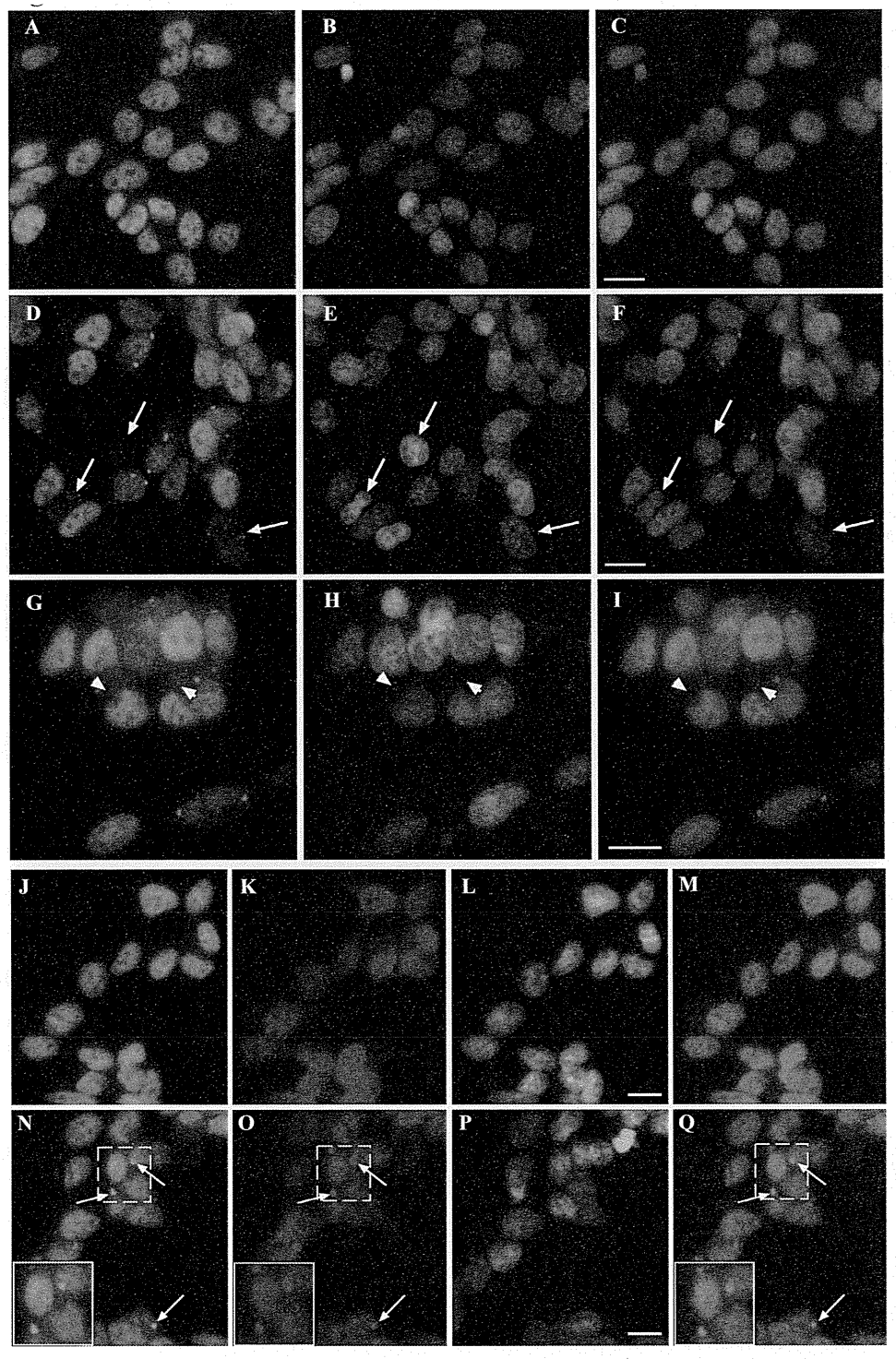

Figure 2 Induction of cytosolic TDP-43 accumulation and SGs by paraquat in SH-SY5Y cells. Cells were exposed overnight to 1 mM paraquat and TDP-43 localization was examined by immunofluorescence. **A-C**: untreated, **D-I**: paraquat treated. Arrows show loss of nuclear TDP-43. Arrowheads show diffuse cytosolic TDP-43. Green = TDP-43, blue = DAPI. Right-hand panels = merged images. **J-Q:** Cells were exposed to 1 mM paraquat overnight and TDP-43 and HuR localization was measured by immunofluorescence. **J-M**: untreated, **N-Q**: paraquat treated. Green = TDP-43, Red = HuR, Blue = DAPI. **M** and **Q** are merged images from TDP-43 and HuR panels. Arrows indicate stress granules. Inset shows higher magnification of TDP-43 and HuR positive SGs. Bar = 10 μm. Representative images from four separate experiments performed in duplicate or triplicate.

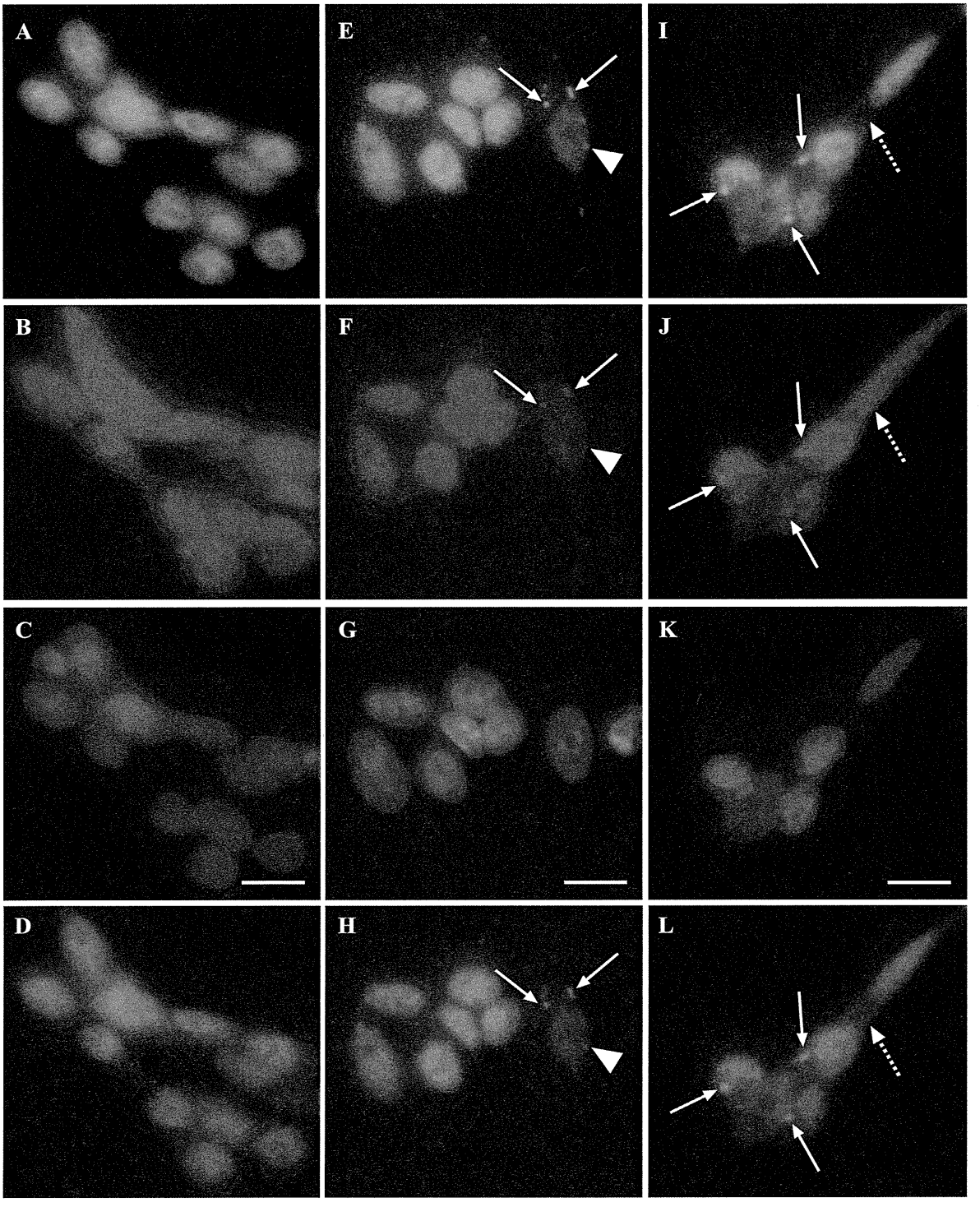

Figure 3 Treatment of SH-SY5Y neurons induces co-localization of TDP-43 and ubiquitin in SGs. Cells were treated overnight with 1 mM paraquat and localization of TDP-43 and ubiquitin was determined by immunofluorescence. **A-D**: untreated, **E-L**: paraquat treated. Green = TDP-43, red = ubiquitin, blue = DAPI. **D**, **H** and **L** represent merged images of panels above. Solid arrows indicate co-localization of TDP-43 and ubiquitin in SGs. Arrowhead indicates lack of co-localization of TDP-43 and ubiquitin in one SG in panel **F**. Dotted arrow indicates lack of co-localization of diffuse TDP-43 and ubiquitin. Bar = 10 μm. Representative images from three separate experiments performed in duplicate or triplicate.

(Additional File 3G). It is possible that more prolonged treatment of cells is required to induce phosphorylation or that the correct cellular kinases are not present or not-localized to SGs. Alternatively the TDP-43 may be phosphorylated on sites different to the 409/410 site. However, the combination of clear nuclear loss of TDP-43, diffuse cytosolic accumulation, aggregation and ubiquitination under mild stress provided a unique model for investigating the early processes in abnormal TDP-43 processing associated with ALS and FTD.

Paraquat induces formation of caspase-dependent and caspase-independent TDP-43 SGs

One of the hallmark neuropathological features of TDP-43 proteinopathies is the formation of C-terminal TDP-43 fragments (CTF-TDP-43), often of 35 or 25 kDa in mass [6,8]. Cell studies have re-capitulated features of end-stage TDP-43 proteinopathies through expression of these fragments which aggregate and co-localize with SG proteins [13,27]. Therefore, we examined if our paraquat model also induced CTF-TDP-43. The SH-SY5Y cells revealed basal expression of a 35 kDa TDP-43 band even in untreated cultures. This is consistent with previous observations [28]. Western blot analysis of paraquat-treated cells revealed the increased expression of this 35 kDa CTF-TDP-43 (Figure 4A). Interestingly, none of the additional mitochondrial inhibitors or nitrosative stress inducers tested significantly elevated 35 kDa CTF-TDP-43 (Figure 4A and 4B). This was despite inducing a similar loss of cell viability (Additional File 1). These findings suggested that formation of TDP-43 SGs may be specifically associated with CTF-TDP-43 as previously supported by studies involving transfection of cells with TDP-43 CTF constructs [16]. Co-treatment of cells with paraquat and the broad-spectrum caspase inhibitor, Z-VAD-fmk, resulted in a complete inhibition of increased 35 kDa CTF-TDP-43 expression (Figure 4C). This supported previous studies demonstrating that 35 kDa TDP-43 CTFs are generated by caspase-cleavage at a DETD consensus site within the NLS of TDP-43 [29,30]. However, we found that while inhibiting CTF-TDP-43 generation with Z-VAD-fmk partially inhibited TDP-43 SG formation (Figure 4H), the effect was not complete. Treatment of cultures with Z-VAD-fmk reduced the number of cells containing TDP-43-positive SGs from 18 ± 8% to 8 ± 2% ($P < 0.05$). This inhibitory effect was mainly due to a reduction in cells containing smaller TDP-43-positive SGs as there was no loss of large (≥ 1 μm) TDP-43 SGs in Z-VAD-fmk treated cells, despite a complete inhibition of enhanced 35 kDa CTF formation. In our cultures, no change was observed to a faint 25 kDa CTF-TDP-43 (Figure 4C), ruling out involvement of this fragment in TDP-43 SG formation. Nishimoto et al. have also reported that the 25 kDa form is not involved in TDP-43 SG formation [30]. These findings strongly suggest that while paraquat treatment enhanced 35 kDa CTF-TDP-43 formation, this was not sufficient for TDP-43 SG formation.

Induction of cytosolic TDP-43 accumulation by paraquat is not mediated through mitochondrial inhibition

As paraquat is a mitochondrial electron transport chain inhibitor, we compared paraquat treatment with alternative inhibitors of cellular respiration to determine if mitochondrial impairment induced TDP-43 SGs. Figure 5P-R shows that only paraquat induced cytosolic accumulation and formation of TDP-43-positive SGs after an overnight treatment. Other mitochondrial inhibitors including rotenone (Figure 5D-F), 3-NP (Figure 5G-I), MPP+ (Figure 5J-L) and sodium azide (Figure 5M-O) had no effect on TDP-43 despite being applied at concentrations that induced the same or increased level of mild cell toxicity (Additional File 1). We then determined if the alternative mitochondrial respiration inhibitors induced HuR-positive SGs that lacked TDP-43. However, as shown in Additional File 4, no HuR-positive SGs were observed in cells after overnight treatment with the mitochondrial inhibitors. These observations showed that the ability of paraquat to induce loss of nuclear TDP-43, cytosolic accumulation and SGs is not solely attributable to its ability to inhibit mitochondrial activity per se. These findings suggest that the effects of paraquat on TDP-43 are more likely associated with specific pathways of oxidative or nitrosative stress induction that differ from the other mitochondrial inhibitors.

JNK controls TDP-43 localization to SGs during oxidative stress

It has been reported previously that kinases can control cytoplasmic localization and SG accumulation of hnRNPs such as hnRNP A1 and hnRNP K. This includes p38, JNK and ERK-dependent modulation of hnRNP sub-cellular accumulation [31-36]. Of these, JNK has been clearly established as a critical stress-activated kinase [37] and is central to toxic effects of paraquat [38,39]. Therefore, we examined if modulation of JNK activity affected TDP-43-positive SG formation. Initially, we determined if paraquat induced activation of JNK and p38 as previously reported [38]. After overnight treatment with 1 mM paraquat robust activation of JNK and ERK was observed with weaker p38 activity (Figure 6A). A time course of activation revealed elevated JNK and ERK phosphorylation after 30-60 min with maximal activation at 2 hr (Figure 6A). No early activation of p38 was observed (data not shown). Subsequent co-treatment of cultures with paraquat and the JNK inhibitor, SP600125, resulted in almost complete inhibition of

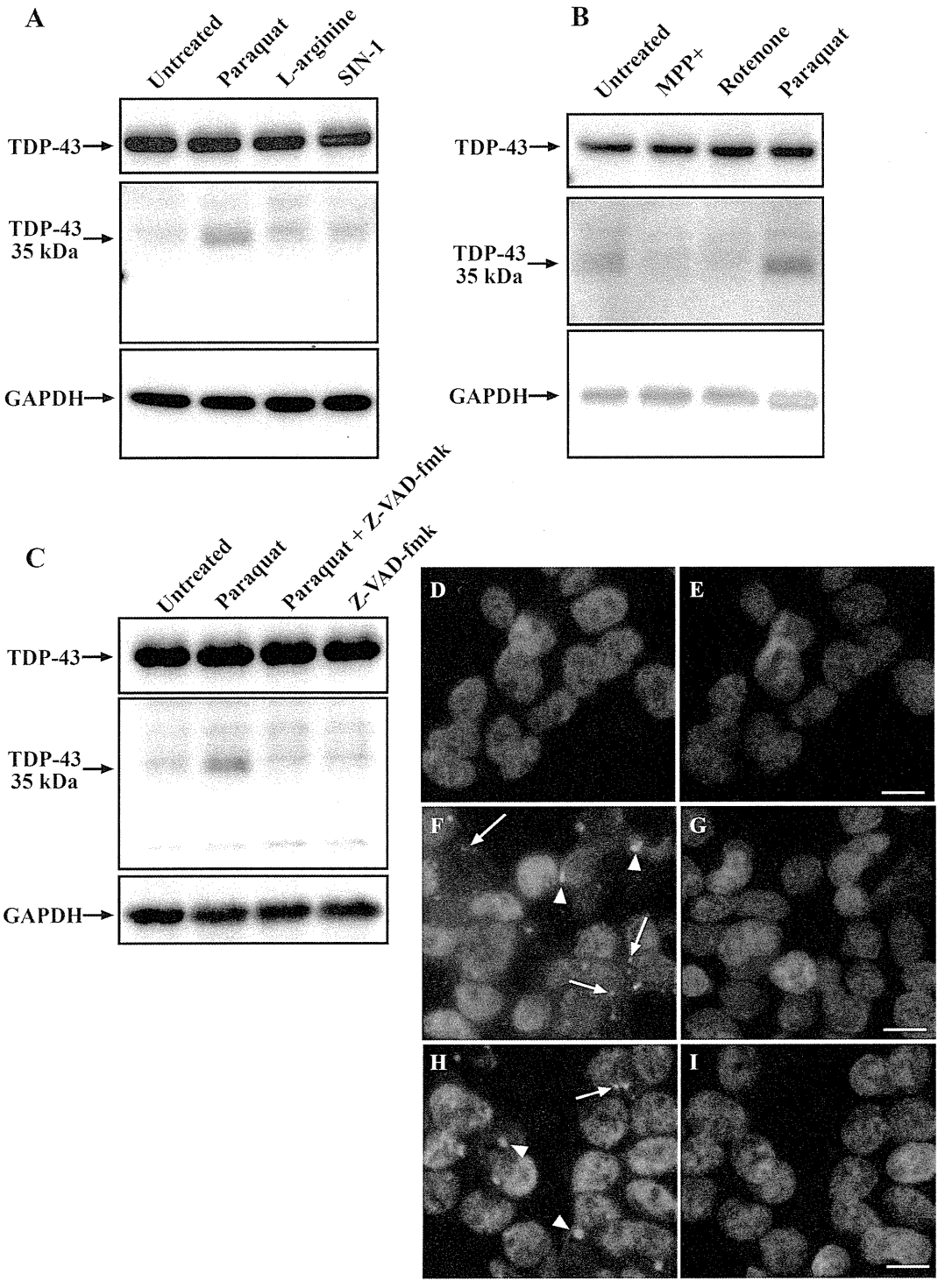

Figure 4 Paraquat treatment induces up-regulation of a caspase-dependent TDP-43 fragment. SH-SY5Y cells were treated overnight with 1 mM paraquat, 1 mM arginine, 100 μM SIN-1 (**A**), or 1 mM paraquat, 2 mM MPP+, 0.075 mM rotenone (**B**) and TDP-43 expression was determined by immunoblot. **C**: Cells were treated overnight with 1 mM paraquat with and without 50 μM Z-VAD-fmk (caspase inhibitor) and TDP-43 expression was determined by immunoblot. Middle panels represent a longer exposure to visualize the 35 kDa band. **D-I:** Cells were treated overnight with paraquat in the absence (**F-G**) and presence (**H-I**) of Z-VAD-fmk and examined for TDP-43-positive SGs. Green = TDP-43, Blue = DAPI. Arrows indicate TDP-43-positive SGs ≤ μm. Arrowheads indicate TDP-43-positive SGs ≥ 1 μm. Bar = 10 μm. Representative images from two-three separate experiments.

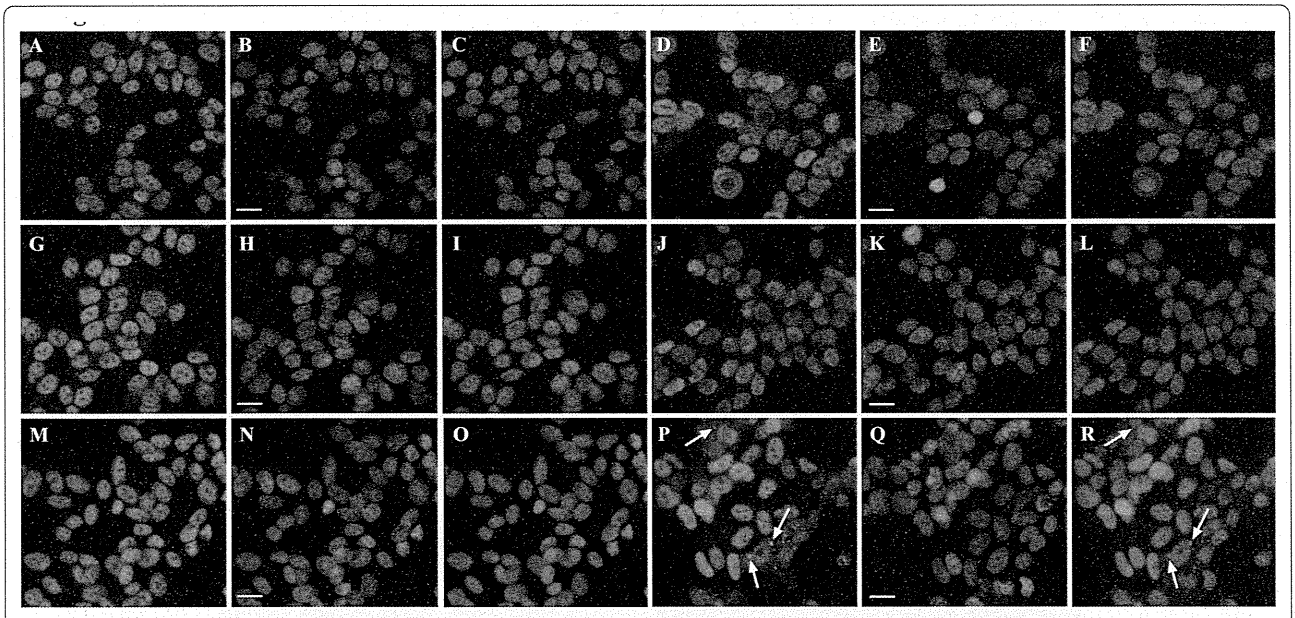

Figure 5 Treatment of SH-SY5Y cells with different mitochondrial inhibitors did not induce TDP-43 aggregation. Cells were treated with vehicle control (**A-C**), 0.075 mM rotenone (**D-F**), 1 mM 3-NP (**G-I**), 2 mM MPP+ (**J-L**), 5 mM sodium azide (**M-O**) or 1 mM paraquat (**P-R**). Cells were analyzed for TDP-43 localization by immunofluorescence. Green = TDP-43, blue = DAPI. C, F, I, L, O and R represent merged images of adjacent TDP-43 and DAPI panels to the left. Arrows indicate TDP-43 SGs in paraquat-treated cells. Bar = 10 μm. Representative images from three separate experiments performed in duplicate or triplicate.

TDP-43-positive SGs, with little effect on the presence of HuR-positive SGs (Figure 6B and 6C-R). This was paralleled by inhibition of JNK phosphorylation (Additional File 4K). The numbers of SGs per cell was used as a more consistent indicator than total number of cells containing SGs. However, in paraquat-treated cultures, the number of cells containing one or more TDP-43-positive SGs was 18 ± 8% of all cells. Co-treatment with SP600125 and paraquat reduced this to 0.22 ± 0.06% of cells ($P < 0.01$). No cells containing SGs were observed in control cultures.

As SP600125 is not entirely specific for JNK, we also tested the effect of BI-78D3, a specific JNK inhibitor on TDP-43 SG formation [40] and found that this induced the same effect as SP600125 (data not shown). This was further supported by the fact that inhibition of another SP600125 target kinase, casein kinase 1 (CK1) with a CK1 inhibitor (D4476), had no effect on TDP-43 or HuR SG formation (Figure 6B). Additional confirmation of the specific role for JNK in TDP-43 accumulation in stress granules was obtained through JNK knockdown. Treatment with combined siRNA against JNK1 and JNK2 significantly reduced JNK expression (Additional File 5A). Subsequent treatment with paraquat resulted in almost no TDP-43-positive stress granules while still inducing HuR-positive stress granules (Additional File 5B-M).

In contrast, inhibition of ERK with PD98059 had a substantial inhibitory effect on both TDP-43 and HuR-positive SG formation (Figure 6B and Figure 7I-L compared to A-D). In paraquat-treated cultures, 27.4 ± 7% of cells contained HuR-positive SGs (no HuR-positive SGs were observed in control cultures). This was reduced to 1.5 ± 0.3% after treatment with PD98059 ($P < 0.01$). A parallel decrease in the number of cells containing TDP-43-positive SGs was observed (reduced from 18 ± 8% to 0.99 ± 0.2% of cells, $P < 0.01$). These effects were also confirmed using the additional ERK inhibitor, U0126 and Raf inhibitor, GW5074 (data not shown). A somewhat weaker effect was observed on TDP-43 and HuR SG formation by SB203580, an inhibitor of p38 (Figure 6B and Figure 7M-P compared to A-D). SB203580 reduced the number of cells containing HuR-positive SGs from 27.4 ± 7% to 12.9 ± 1.7% ($P < 0.01$) and cells containing TDP-43-positive SGs from 18 ± 8 to 7.2 ± 2.1% ($P < 0.01$). Although ERK was activated earlier than p38 by paraquat, the inhibition of HuR and TDP-43-positive SGs by inhibitors of both kinases is consistent with our observations that SGs were not detected until after 8 hr of paraquat exposure (data not shown). This suggests that different kinases may have a role in SG formation over the prolonged exposure to paraquat with JNK controlling TDP-43 association and ERK and p38 affecting TDP-43 and

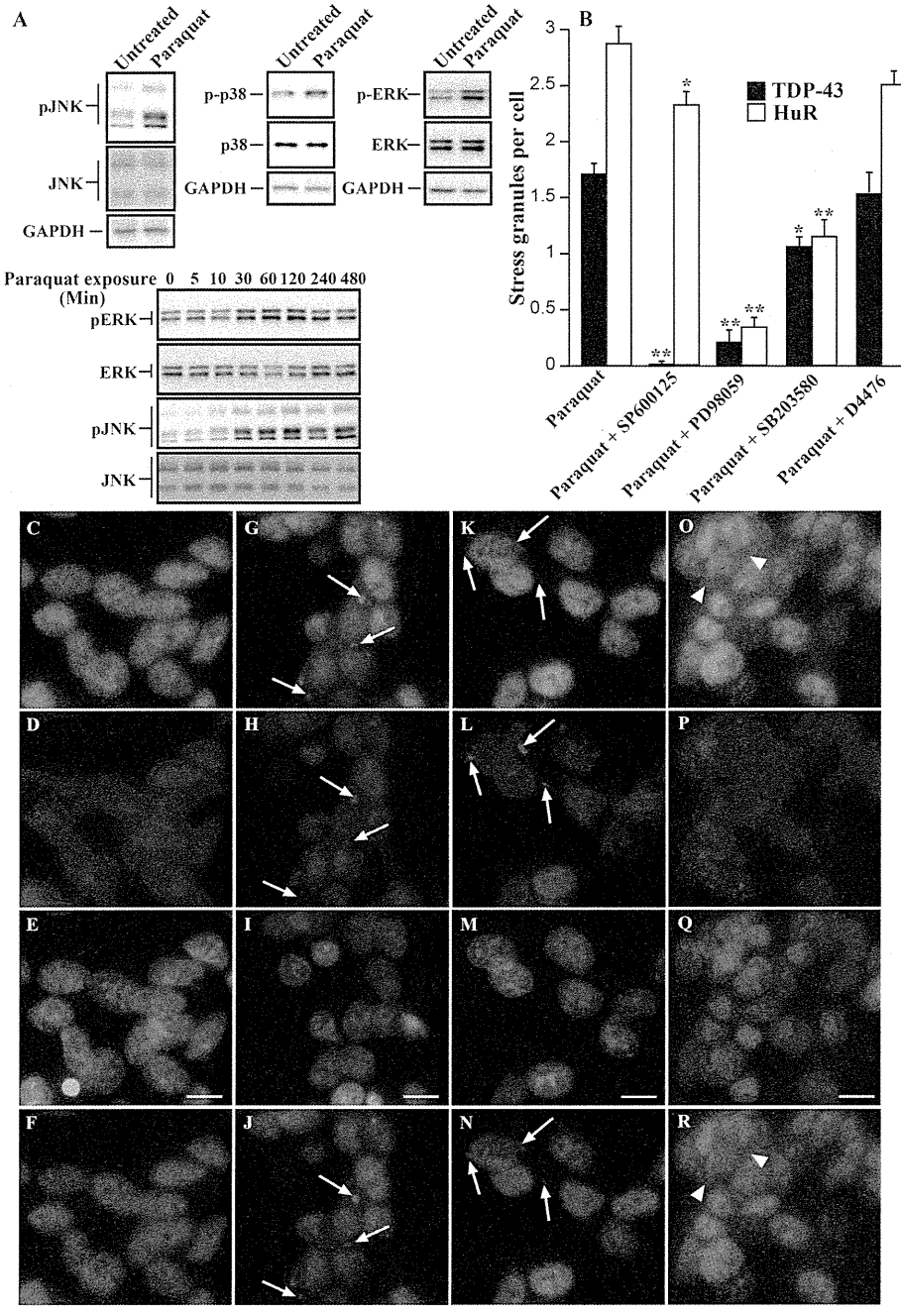

Figure 6 Treatment of SH-SY5Y cells with paraquat induces JNK-dependent accumulation of TDP-43 into SGs. Cells were treated with 1 mM paraquat overnight. Where indicated, cells were co-treated with 10 μM SP600125 (JNK inhibitor), PD98059 (ERK inhibitor), SB203580 (p38 inhibitor) or D4476 (CK1 inhibitor). Cells were examined for phosphorylation of kinases by immunoblot and accumulation of TDP-43 and HuR by immunofluorescence. **A**: Cells were treated with paraquat and examined after overnight incubation for activation of JNK, p38 and ERK. In addition, cells were incubated with paraquat and examined at different time points from 0-480 min (8 hr) for ERK and JNK activation. Lower panels for each image indicate that total kinase expression is unchanged, upper panels indicate changes to phorphorylated forms. **B**: Cells were treated with paraquat in the presence or absence of kinase inhibitors and the number of TDP-43 and HuR SGs was determined. *$p < 0.05$, **$p < 0.01$. n = minimum of 500 cells counted across multiple coverslips and separate experiments for each inhibitor. **C-F**: Untreated, **G-J**: Paraquat treated, **K-N**: Paraquat + SP600125 showing loss of TDP-43 but not HuR SGs, **O-R**: Paraquat + SP600125 showing loss of TDP-43 SGs but not diffuse cytosolic TDP-43. Green = TDP-43, red = HuR, blue = DAPI. Bottom panels indicate merged images of TDP-43 and HuR panels above. Arrows indicate SGs, arrowheads indicate diffuse TDP-43. Bar = 10 μm. Representative images from two-four separate experiments performed in duplicate or triplicate.

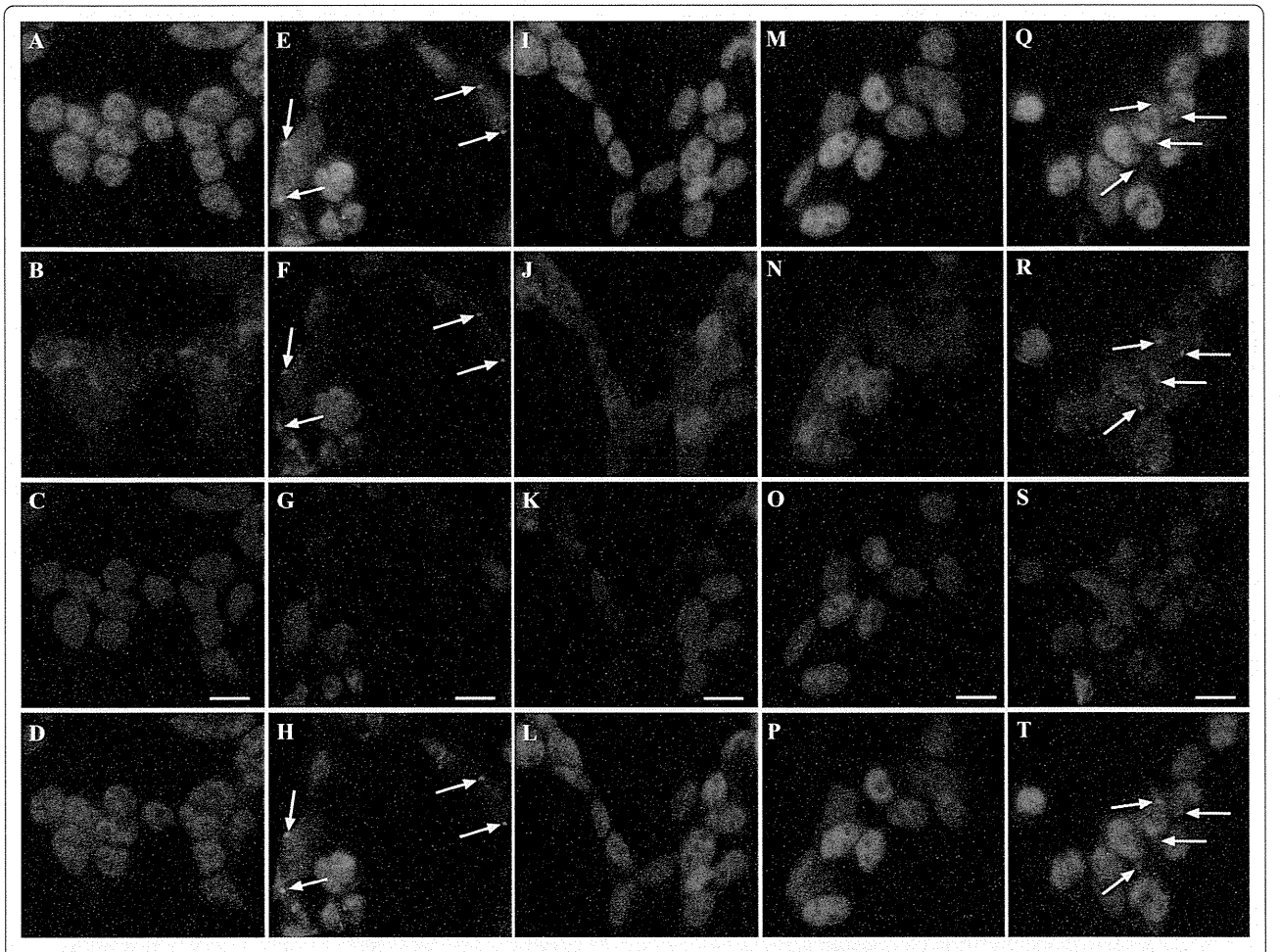

Figure 7 Treatment of SH-SY5Y cells with paraquat induces ERK and p-38-dependent accumulation of TDP-43 and HuR-positive SGs. Cells were treated overnight with 1 mM paraquat in the absence or presence of 10 μM PD98059 (ERK inhibitor), SB203580 (p38 inhibitor) or SP600125 (JNK inhibitor) and immunofluorescence analysis of TDP-43 and HuR was performed. **A-D:** Untreated control, **E-H:** paraquat-treated, **I-L:** paraquat and PD98059, **M-P:** paraquat and SB203580, **Q-T:** paraquat and SB600125. Green = TDP-43, red = HuR, blue = DAPI. Arrows indicate SGs. Bottom panel indicates merged images from TDP-43 and HuR panels above. Bar = 10 μm. Representative images from three separate experiments performed in duplicate or triplicate.

additional SG protein accumulation. This is the first report of JNK and additional kinases controlling TDP-43 localization to SGs. The fact that inhibition of JNK resulted in almost complete abrogation of TDP-43-positive SGs with little effect on HuR localization to SGs indicated that JNK is potentially a key controller of TDP-43 (and possibly other hnRNP) association with SGs rather than simply mediating SG formation *per se*.

As the majority of studies on SGs involve acute (0.5 - 1 hr) treatment with toxic doses of stress inducers such as arsenite, heat shock or osmotic stress, we examined whether a short-term treatment with paraquat induced JNK-controlled TDP-43 SG formation. Interestingly treatment of cells for 1 hr with up to 5 mM paraquat had no effect on HuR or TDP-43 (data not shown), demonstrating that paraquat-mediated SG formation is a longer term process requiring prolonged incubation for TDP-43 to localize to SGs. The data are more consistent with a role for paraquat in prolonged oxidative stress than impairment of mitochondrial function and suggest that paraquat or other chronic inducers of TDP-43 SG formation may provide useful models to mimic the slow progression of disease-associated changes in ALS or FTD.

JNK controls TDP-43 SG association in different cell-types

To determine if the effect of JNK inhibition on TDP-43 localization with SGs in SH-SY5Y cells was specific for this cell-type, we compared this to additional cell-lines treated with paraquat. Treatment of HeLa cells and U87MG glial cells overnight with 1 mM paraquat resulted in TDP-43-positive SGs (Additional File 6). Extensive numbers of TDP-43 SGs were observed in HeLa cells (~28% of cells) while SG positive cells in

U87MG cultures were rare (~2% of cells) (Additional File 6). No paraquat-induced SGs were observed in HEK293 or human fibroblasts (GSM2069) (not shown). Co-treatment of HeLa cultures with paraquat and SP600125, dramatically reduced formation of TDP-43-postive SGs, with only a limited effect on the presence of HuR-positive SGs analogous to SP600125 treatment of SH-SY5Y cells (data not shown). These findings demonstrate that paraquat induces TDP-43-positive SGs in different cell-types and JNK-mediated control of TDP-43 with SGs is not specific for one cell line but appears to be a consistent feature of chronic stress-induced SG formation.

JNK partially controls TDP-43 association with SGs in arsenite stress

We examined whether inhibition of JNK also affected localization of TDP-43 in cells exposed to sodium arsenite, the most commonly used SG inducer. Sodium arsenite is also known to induce JNK activation [41]. Initially, we compared the effect of sodium arsenite on TDP-43 in SH-SY5Y cells at a concentration that induced the same level of toxicity as paraquat did overnight. 50 μM sodium arsenite overnight induced 58% cell viability (compared to 57% cell viability in cells treated with 2 mM paraquat overnight, Additional File 1B). However, this level of toxicity with sodium arsenite did not cause cytosolic TDP-43 SGs. We also examined short term treatment of cells with sodium arsenite (0.5 mM sodium arsenite for 1 hr) and while this induced robust HuR SGs, few cells revealed TDP-43 co-localization. Given the lack of TDP-43 SGs in the sodium arsenite-treated SH-SY5Y cells, we treated HeLa cells with sodium arsenite (0.5 mM 1 hr). This treatment induced widespread TDP-43 and HuR-positive SGs (Figure 8D-F). To determine if JNK activity was responsible for TDP-43 accumulation in sodium arsenite-treated cells, cultures were co-treated with SP600125 and paraquat. Interestingly, we observed a 46% decrease in the number of cells positive for TDP-43 SGs (Figure 8G-I). As with inhibition of paraquat-treated SH-SY5Y cells, SP600125 had little effect on HuR SGs (Figure 8G-I). This partial, but significant, inhibition of TDP-43 localization to SGs by JNK inhibition suggests that JNK has a role in TDP-43-SG interaction during acute sodium arsenite treatment but other factors (e.g. other kinases) are also involved.

JNK inhibition partially modulates aggregation of transfected CTF-TDP-43

Next we investigated whether JNK controls aggregation of transfected CTF-TDP-43 constructs. SH-SY5Y cells were transfected with GFP-tagged vector control, full length TDP-43, CTF-TDP-43 162-414 or CTF-TDP-43 219-414 for 48 hrs. As expected, no aggregates of TDP-43 were observed in cells exposed to vector control (Figure 9A-B) or full length TDP-43 (Figure 9C-D). In contrast, CTF-TDP-43 162-414 or 219-414 induced cytoplasmic aggregates in cells after 48 hr consistent with previous reports [15] (Figure 9E-F and 9I-J). We then treated cultures with SP600125 after 24 hr (to allow transfection to stabilize) and examined the formation of TDP-43 aggregates after a further 24 hr incubation. While treatment with SP600125 did not reduce the number of cells containing aggregated TDP-43, there was a significant decrease in the number of aggregates per cell in cultures transfected with TDP-43 162-414 (Figure 9K-L and 9M) and 219-414 (Figure 9G-H and 9M). ERK inhibition induced a small decrease in number of aggregates but this was not significant. These findings suggested that the aggregation of these CTF-TDP-43 fragments maybe partially affected by JNK. This could be due to a role for basal JNK activity in modulating CTF-TDP-43 aggregation or alternatively, early aggregation of the CTF-TDP-43 fragments could induce cell stress that promotes further CTF-TDP-43 aggregation via JNK activation. This stress may then accelerate aggregation in some cells.

JNK inhibition of TDP-43 SG formation is not due to inhibition of 35 kDa CTF-TDP43 expression

Interestingly, while JNK inhibition blocked TDP-43 incorporation in SGs, it did not have a substantial effect on inhibiting accumulation of diffuse cytosolic TDP-43 or prevent loss of nuclear TDP-43 induced by paraquat treatment (Figure 6C-R). This finding provided further support for the role of JNK in modulating cytosolic TDP-43 incorporation into SGs rather than affecting upstream processes leading to loss of nuclear TDP-43 and accumulation of TDP-43 in the cytosol. Additional support for this was obtained when we examined the effect of JNK inhibition on 35 kDa CTF-TDP-43 accumulation. As shown in Figure 10, co-treatment of cultures with the JNK inhibitor, actually led to an increase in detectable levels of the 35 kDa CTF-TDP-43 rather than inhibit its formation. This is consistent with the data in Figure 4 demonstrating that the formation of TDP-43-positive SGs was not fully prevented by inhibiting 35 kDa CTF-TDP-43 formation using a caspase inhibitor.

JNK inhibition blocks association of hnRNP K and TDP-43 with SGs

In order to obtain an insight into the potential mechanism by which JNK controls TDP-43 association with SGs during chronic stress, we examined co-localization with other hnRNPs. Previous studies have reported that TDP-43 binds to hnRNPs including hnRNP A1 and K